

Fluorescence Lifetime Imaging in Stargardt Disease: Potential Marker for Disease Progression

Chantal Dysli,¹ Sebastian Wolf,¹ Katja Hatz,^{2,3} and Martin S. Zinkernagel¹

¹Department of Ophthalmology and Department of Clinical Research, Inselspital, Bern University Hospital and University of Bern, Bern, Switzerland

²Vista Klinik, Binningen, Switzerland

³University Hospital Basel, Basel, Switzerland

Correspondence: Martin S. Zinkernagel, University Hospital Bern, 3010 Bern, Switzerland; m.zinkernagel@gmail.com.

Submitted: August 24, 2015

Accepted: December 29, 2015

Citation: Dysli C, Wolf S, Hatz K, Zinkernagel MS. Fluorescence lifetime imaging in Stargardt disease: potential marker for disease progression. *Invest Ophthalmol Vis Sci.* 2016;57:832–841. DOI:10.1167/iovs.15-18033

PURPOSE. The purpose of this study was to describe autofluorescence lifetime characteristics in Stargardt disease (STGD) using fluorescence lifetime imaging ophthalmoscopy (FLIO) and to investigate potential prognostic markers for disease activity and progression.

METHODS. Fluorescence lifetime data of 16 patients with STGD (mean age, 40 years; range, 22–56 years) and 15 age-matched controls were acquired using a fluorescence lifetime imaging ophthalmoscope based on a Heidelberg Engineering Spectralis system. Autofluorescence was excited with a 473-nm laser, and decay times were measured in a short (498–560 nm) and long (560–720 nm) spectral channel. Clinical features, autofluorescence lifetimes and intensity, and corresponding optical coherence tomography images were analyzed. One-year follow-up examination was performed in eight STGD patients. Acquired data were correlated with in vitro measured decay times of all-*trans* retinal and *N*-retinylidene-*N*-retinylethanolamine.

RESULTS. Patients with STGD displayed characteristic autofluorescence lifetimes within yellow flecks (446 ps) compared with 297 ps in unaffected areas. In 15% of the STGD eyes, some flecks showed very short fluorescence lifetimes (242 ps). Atrophic areas were characterized by long lifetimes (474 ps), with some remaining areas of normal to short lifetimes (322 ps) toward the macular center.

CONCLUSIONS. Patients with recent disease onset showed flecks with very short autofluorescence lifetimes, which is possible evidence of accumulation of retinoids deriving from the visual cycle. During the study period, many of these flecks changed to longer lifetimes, possibly due to accumulation of lipofuscin. Therefore, FLIO might serve as a useful tool for monitoring of disease progression. (ClinicalTrials.gov number, NCT01981148.)

Keywords: fluorescence lifetimes, fundus autofluorescence, ophthalmic imaging, Stargardt disease, STGD, fundus flavimaculatus, retinal dystrophies, FLIO

Stargardt disease (STGD) is an autosomal recessive disease with a prevalence of approximately 1:10,000.^{1,2} It is the most common form of hereditary, recessive macular dystrophy and is characterized by reduced visual acuity and central vision loss with onset in childhood or early adulthood.^{3,4} The clinical appearance is characterized by yellow flecks at the level of the RPE distributed around the macula and the midperiphery of the posterior pole.² Additionally, in later stages of disease, there is progressive bilateral atrophy of the RPE resembling geographic atrophy in age-related macular degeneration. In the majority of patients (80%), the disease is caused by a mutation in the ATP-binding cassette transporter (ABCA4) gene, located within chromosome 1p13.^{5–8} ABCA4 encodes for the ABCA4 receptor (ABCR), which is a photoreceptor-specific adenosine triphosphate-binding cassette transporter. ABCR acts as a phospholipid flippase within the rims and incisures of cone and rod outer segments, enabling vitamin A derivatives to be transported through the outer segment disc membranes.⁹ Dysfunctional ABCR leads to abnormal lipofuscin accumulation within the RPE.^{10–12} Lipofuscin is a byproduct of the visual cycle degradation and

consists of various fluorophores including *N*-retinylidene-*N*-retinylethanolamine (A2E).¹³ Fundus autofluorescence (FAF) has been established as a tool to visualize lipofuscin components in vivo^{10,14} and has significantly promoted our understanding of the pathophysiology of retinal dystrophies.^{15,16} However, it is still disputed which specific components of the visual cycle lead to an increase in FAF. A recent study using mass spectrometry has shown that A2E is predominantly distributed toward the periphery of the retina and does not correlate with lipofuscin distribution and thereby may not contribute to the increase in FAF levels within the macular center in physiologic aging conditions.¹⁷ Furthermore, increased FAF observed in the border zone of geographic atrophy in age-related macular degeneration has been attributed to formation of stacked RPE cells and not primarily to lipofuscin accumulation within individual cells.^{18,19} The FAF in STGD is characterized by a general increase of autofluorescence intensity, particularly in the short wavelengths, at early stages of the disease.¹¹ With advanced disease, well-demarcated hyperautofluorescent lesions corresponding to the visible yellowish flecks appear.^{20–22} Further-



TABLE 1. Demographical and Clinical Data

Characteristics	Stargardt		Control		P Value
	Mean	SEM	Mean	SEM	
Number	16	—	15	—	
Sex, F, M	9, 7		9, 6		
Age, y	40.25	2.53	40.73	2.37	0.94
Age range, y	22–56	—	25–58	—	
Age of onset, y	29.00	2.23	—	—	
BCVA, ETDRS letters	55.84	4.15	85.87	0.29	<0.0001
Phenotype, Fishman classification	1.94	0.12	—	—	

Summary of demographic and clinical data from all Stargardt patients and healthy controls included in this study.

more, in the later stages of STGD, there is marked hypoautofluorescence in the area of atrophic changes, usually located at the posterior pole.^{23,24}

Fundus autofluorescence can not only be quantified by measuring the fluorescence intensity but also by measuring the time a molecule spends in the excited state before returning to the ground state. Autofluorescence decay times of endogenous fluorophores can be measured after excitation with a laser.²⁵ The technique of fluorescence lifetime imaging ophthalmoscopy (FLIO) has been shown to be reproducible, noninvasive, and easily deployable in a clinical setting.^{26,27}

Several therapies for STGD, such as gene replacement therapy and stem cell transplantation, are currently being assessed in human trials. Evaluating potential therapies may be difficult because reliable readouts for short-term effects are currently lacking. Parameters, such as visual acuity or microperimetry, have been used to monitor therapeutic effects, but may be fraught with bias due to their subjective nature. Therefore, an objective readout to assess short-term progression of STGD may be helpful to assess novel treatment approaches.

The purpose of this study was to perform an extensive clinical characterization of STGD patients using a fluorescence lifetime ophthalmoscope and correlate these findings with optical coherence tomography (OCT) and functional parameters.

METHODS

Patients and Healthy Controls

A total of 32 eyes of 16 patients with a clinical diagnosis of STGD were included in this study (56% female). A cohort of 15 age-matched healthy subjects with no ophthalmic diseases was used as a control group (60% female). The mean age was 40.3 ± 10.1 years (SD) for the Stargardt group and 40.7 ± 9.2 years (SD) for the controls ($P = 0.94$). All participants were Caucasian and phakic and did not have any concomitant ophthalmic disease (patient characteristics are shown in Tables 1, 2).

According to their phenotypic appearance on color and FAF images, all Stargardt patients were assigned to one of three groups from the Fishman classification.²⁸ In Fishman I, retinal abnormalities as flecks and atrophic areas are restricted to the macular center; in Fishman II, flecks are spread throughout the posterior pole, extending anterior to the vascular arcades and/or nasal to the optic disc; and Fishman III has “resorbed” flecks and widespread atrophy of the RPE.

Fifty percent of the patients were examined twice after a 12-month follow-up interval to assess disease activity and progression.

All participants underwent a general ophthalmologic examination, and best corrected visual acuity (BCVA; Early Treatment Diabetic Retinopathy Study [ETDRS] letters) was measured. Tropicamid 0.5% and phenylephrine HCl 2.5% was

TABLE 2. Patient Characteristics

Patient Number	Sex	Age, y	Age of Onset, y	Visual Acuity		Phenotype		Atrophy		Follow-Up
				Right	Left	Right	Left	Right	Left	
S1	Female	42	35	82	80	2	2	—	—	FU
S2	Male	33	30	79	84	2	2	—	—	FU
S3	Male	53	40	41	36	2	2	—	—	FU
S4	Female	43	12	32	34	3	3	A	A	FU
S5	Female	33	28	75	28	1	1	—	—	
S6	Male	54	34	43	47	2	2	—	—	
S7	Male	45	18	21	21	3	3	A	A	FU
S8	Female	45	40	78	83	2	2	—	—	FU
S9	Female	43	37	73	60	2	2	—	A	FU
S10	Female	56	33	37	34	2	2	A	A	
S11	Female	47	42	85	85	1	1	—	—	FU
S12	Male	22	22	85	73	2	2	—	—	
S13	Female	30	24	57	75	1	1	—	—	
S14	Male	41	18	37	37	2	2	A	A	
S15	Male	31	28	70	53	3	3	—	—	
S16	Female	26	23	42	20	1	1	—	—	

Patient number, sex, age, age of onset, BCVA (ETDRS letters), fundus phenotype 1–3 according to Fishman classification, presence of areas with geographic atrophy (A), 1-year follow-up (FU). Patients S4, S7, and S14 were siblings.

used for maximal pupil dilation. Fluorescence lifetime images, fundus color images (Zeiss FF 450plus; Zeiss, Oberkochen, Germany), and OCT scans of the macula (Heidelberg Spectralis HRA+OCT; Heidelberg Engineering, Heidelberg, Germany) of both eyes were obtained.

This prospective study was conducted at the University Hospital in Bern, Bern, Switzerland, with the approval of the local ethics committee and in accordance with the Declaration of Helsinki. Informed consent was obtained from all participants before study entry. This study is registered at ClinicalTrials.gov as "Measurement of Retinal Auto Fluorescence with a Fluorescence Lifetime Imaging Ophthalmoscope (FLIO Group)," with the identifier number NCT01981148.

Fluorescence Lifetime Imaging Ophthalmoscope

A fluorescence lifetime imaging ophthalmoscope was used for acquisition of retinal fluorescence lifetime data. It is based on a HRA Spectralis system (Heidelberg Engineering). Basic principles of the FLIO technique have been described in a previous study.²⁶ Here, only a brief overview of the technique will be provided.

Retinal autofluorescence was excited using a 473-nm pulsed laser and raster-scanning the central fundus with a repetition rate of 80 MHz.

The laser safety calculations were provided by Heidelberg Engineering and were done according to the International Electrotechnical Commission (IEC) 60825-1:2007.²⁹ This IEC standard is a recognized consensus standard and equals to the American National Standard for the Safe Use of Lasers (ANSI) norm z136, which is only a national standard and not applicable internationally.³⁰ The following three different accessible emission limits (AELs) have been taken into account: (1) the exposure from any single pulse within a pulse train shall not exceed the AEL for a single pulse; (2) the average power for a pulse train of emission duration T shall not exceed the power corresponding to the AEL for a single pulse of duration T (with a thermal and a photochemical limit); and (3) for constant pulse energy and pulse duration, the energy per pulse shall not exceed the AEL for a single pulse multiplied by the correction factor $C5$ (for detailed calculations, see Supplementary Material S1). Thereby, in the scanning beam within the FLIO system, the accessible emission is below class I accessible emission limits.

The emitted fluorescence photons were detected by highly sensitive hybrid photon-counting detectors (HPM-100-40; Becker&Hickl, Berlin, Germany) in a short (498–560 nm; SSC) and in a long (560–720 nm; LSC) spectral channel and registered by time-correlated single-photon counting (TCSPC) modules (SPC-150; Becker&Hickl). An infrared reflectance image allows for tracking of eye movements and data accumulation over the entire acquisition duration of approximately 90 seconds. Becker&Hickl software (SPCImage 4.6) was used for analysis of the recorded lifetime values. The recorded single photons of the fluorescence decay were fitted with a bi-exponential decay function and a binning factor of 1 for each pixel in both the SSC and LSC. The double-exponential approximation of the fluorescence decay curve resulted in a mean decay trace that is characterized by a short decay component $T1$ with its relative amplitude (=relative intensity) $\alpha1$ and a long decay component $T2$ with its relative amplitude $\alpha2$, whereby $T1 \ll T2$ and $\alpha1 \gg \alpha2$. The tau values $T1$ and $T2$ and the amplitudes $\alpha1$ and $\alpha2$ were then used for calculation of the mean fluorescence lifetime Tm .

$$Tm = \frac{\alpha1 * T1 + \alpha2 * T2}{\alpha1 + \alpha2} \quad (1)$$

Tm represents the amplitude weighted mean fluorescence decay time per pixel and wavelength channel.

Fluorescence Lifetime Data Analysis

The custom-made FLIO reader (ARTORG Center for Biomedical Engineering Research, University of Bern, Bern, Switzerland) was used for analysis of the mean retinal fluorescence lifetime values within the areas of a standard ETDRS grid.²⁶ The ETDRS circle diameters were 1 mm for the central area, 3 mm for the inner ring, and 6 mm for the outer ring. For detailed analysis of specific retinal findings, mean fluorescence lifetime values were averaged within an area with circle diameter of 0.16 mm. This small circle was always placed within the area of the inner ring of the standard ETDRS grid. For each single value, the average of at least three independent measurements was taken.

In Vitro Measurements of Fluorescence Lifetimes

In vitro analysis of retinal and A2E were performed. All-trans retinal (atRAL; Sigma-Aldrich, St. Louis, MO, USA) was dissolved in ethanol (1 mg/mL). The sample was measured within a glass test tube. The A2E was kindly provided by Janet R. Sparrow (Department of Ophthalmology, Columbia University, New York, NY, USA). A 200 μ M solution was prepared using methanol as dissolver. The A2E suspension was spread on a glass chamber slide, and methanol was evaporated before measurement. The samples were mounted on a porcelain plate to avoid any background fluorescence, and FLIO measurement was performed in a totally dark room. Data were analyzed in both spectral channels using a binning factor of 5.

Statistical Analysis

Results are presented as mean \pm SEM. Mean values are compared by Mann-Whitney test (two-tailed, confidence interval 95%, significance level = 0.05). Statistical data analysis was performed using Graph Pad Prism version 6 (GraphPad Software, Inc., La Jolla, CA, USA). A stepwise forward regression analysis was performed using SigmaPlot Version 12.3 (Systat Software, Inc., San Jose, CA, USA).

RESULTS

All 16 patients included in this study showed typical clinical features of STGD, with well-defined hyperautofluorescent flecks distributed around the macular center, spreading toward the periphery. Twenty-eight percent of the eyes displayed various degrees of areas with retinal atrophy, appearing black in the autofluorescence measurement. Patient characteristics are summarized in Tables 1 and 2.

Fundus Autofluorescence Lifetimes in Patients With STGD

The fluorescence lifetimes of the fundus in patients with STGD were in the range of age-matched healthy controls (SSC: 246 ± 5 ps, range 219–312 ps, $P = 0.38$; LSC: 297 ± 8 ps, range 226–401 ps, $P = 0.19$). Hyperfluorescent flecks and atrophic areas were clearly discernible in FLIO. Both areas were characterized by both short and long autofluorescence lifetime values (Figs. 1, 2, 3A).

Autofluorescence Lifetimes Analysis in Hyperfluorescent Flecks

Yellowish appearing flecks in the fundus examination corresponded to hyperfluorescent areas in the fundus autofluorescence intensity images of both spectral channels (Fig. 1). In lifetime measurements, flecks were clearly identifiable in both channels as well. In the FLIO images, these areas were

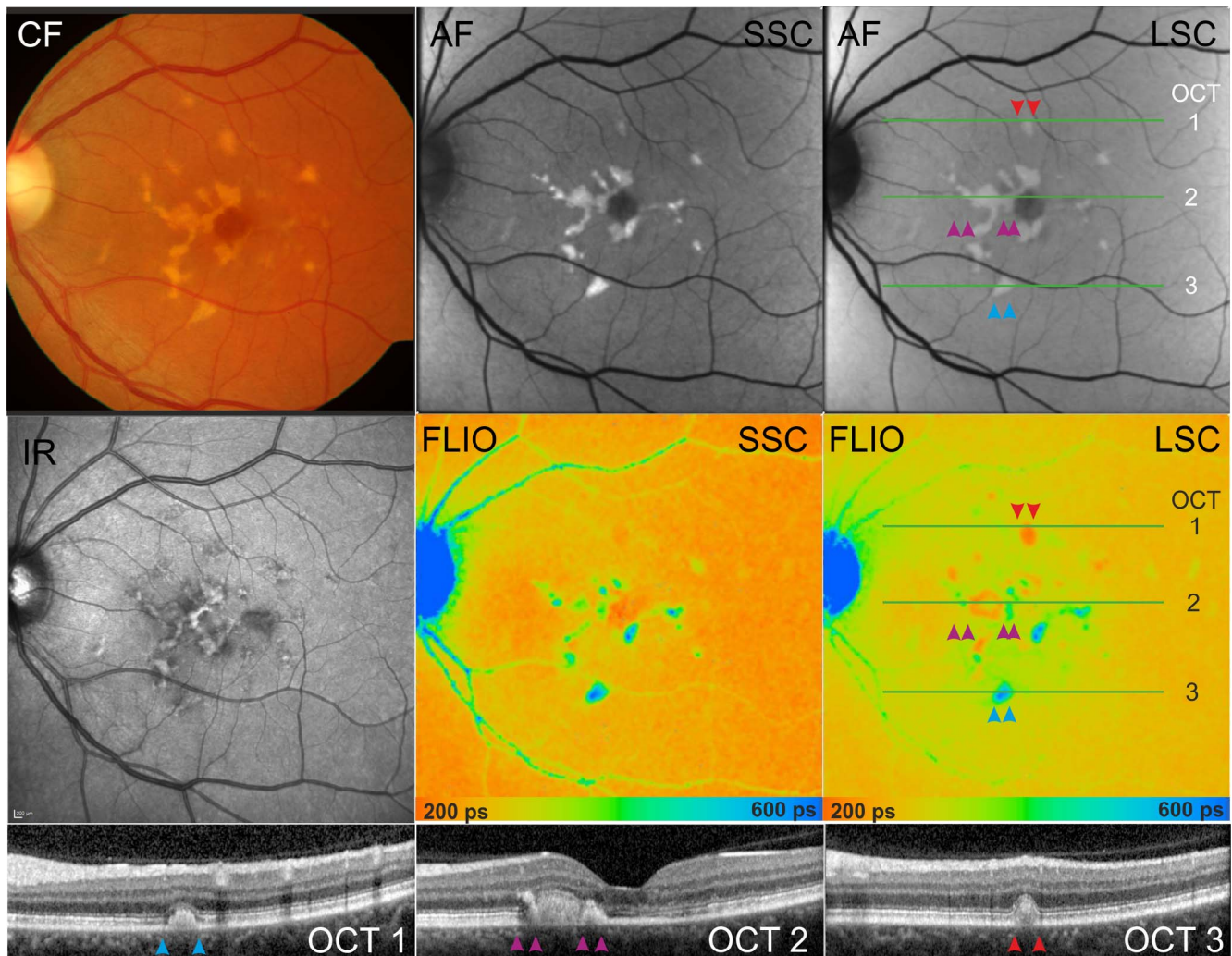


FIGURE 1. Fundus autofluorescence lifetime map of the left eye of a patient with STGD (patient 11). Fundus AF and FLIOs in the short and long spectral channel (SSC = 498–560 nm, LSC = 560–720 nm) with corresponding color fundus (CF), infrared (IR), and optical coherence tomography (OCT 1–3) images. Corresponding locations in AF, FLIO, and OCT are marked with respective *arrowheads*.

characterized by fluorescence lifetimes, which in the majority (85% of the eyes) exhibited solely prolonged fluorescence lifetimes (SSC: 441 ± 10 ps; LSC: 446 ± 8 ps). In 15% of the eyes, additional flecks with shorter fluorescence lifetimes than the surrounding tissue were identified (SSC: 262 ± 14 ps; LSC: 242 ± 4 ps). The discrimination between short and long lifetime flecks was better in the LSC (Fig. 1). Flecks with short lifetimes (red) seemed to be less hyperreflective in OCT than those with long lifetimes (blue). Furthermore, red flecks were predominantly seen in patients with just recent onset of visual symptoms and an active disease progression with progressive metamorphopsia and vision loss.

In the FLIO maps, additional areas with changes in fluorescence lifetime values were clearly identifiable, which were not detectable in autofluorescence intensity or color fundus images (Figs. 1, 2, 4).

Autofluorescence Lifetimes Analysis in Atrophic Areas

Atrophic areas, which are characterized by strongly decreased fluorescence intensity, showed fluorescence lifetimes between 165 and 323 ps (256 ± 15 ps) in the SSC and between 253 and 374 ps (323 ± 15 ps) in the LSC (Fig. 2). There was no

morphologic correlation between areas with short and long fluorescence lifetimes and corresponding areas in the OCT.

Autofluorescence Lifetimes Analysis in Different Fishman Classification Groups

From the total of 32 eyes, 8 eyes (25%) were assigned to Fishman I, 18 eyes (56%) to Fishman II, and 6 eyes (19%) to Fishman III. In this study population, in eyes with Fishman I, no patient showed atrophic areas, whereas in patients with Fishman III, no “normal retina” could be analyzed. Short lifetime flecks were only seen in patients with Fishman I.

Regression Analysis

Stepwise forward regression analysis was performed and included the following factors: diagnosis of STGD, age, sex, Fishman score, and the dependent variables mean fluorescence lifetime (T_m) in the SSC and the LSC. When analyzing mean fluorescence lifetime values within the entire inner ETDRS ring, the diagnosis of STGD (SSC: $P < 0.001$; LSC: $P = 0.012$) and age (SSC: $P < 0.001$; LSC: $P = 0.004$) significantly added to the ability of the equation to predict lifetimes in the SSC or LSC. However, when analyzing contained areas of retina

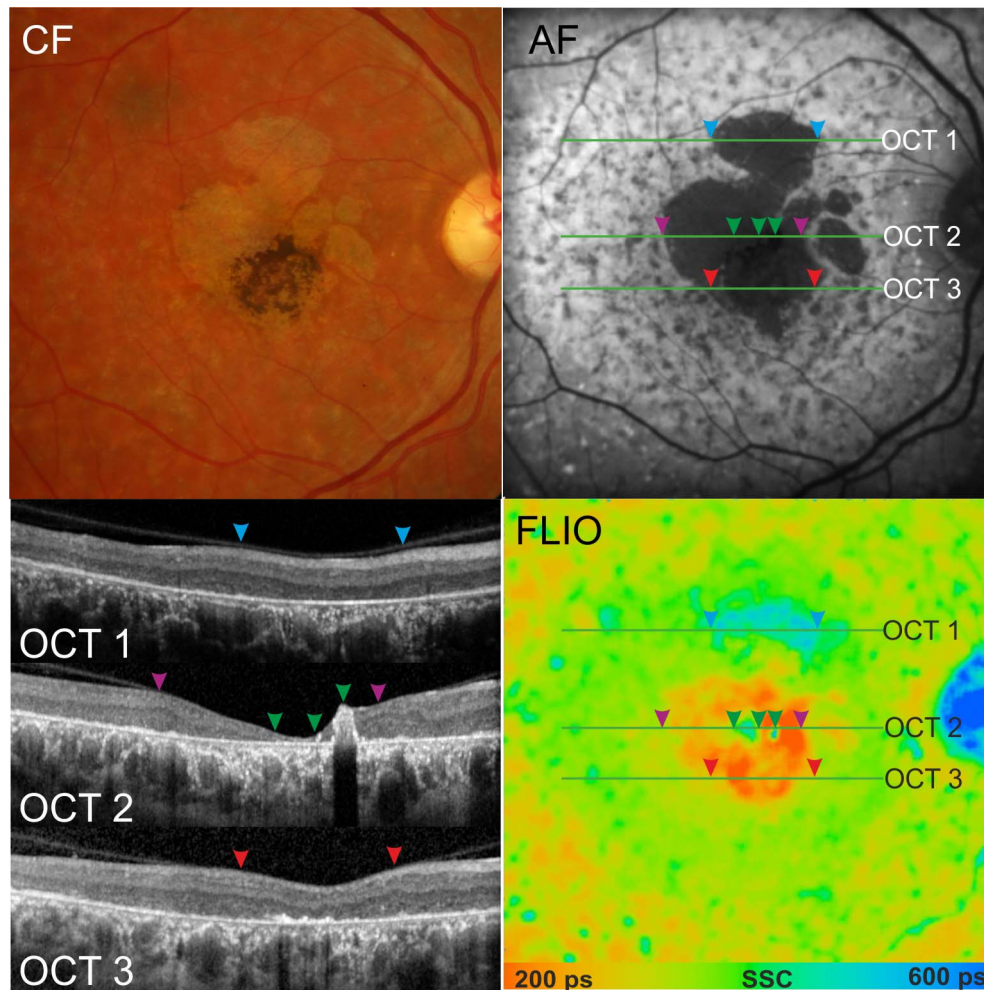


FIGURE 2. Stargardt disease (Fishman III) with central retinal atrophy and pigment accumulation (patient 4). Color fundus (CF), fundus AF, and FLIO (short spectral channel) with indicated lines of the optical coherence tomography sections OCT 1–3. Corresponding locations in AF, FLIO, and OCT are marked with respective *arrowheads*.

not affected by STGD-like changes, only age was identified as a predictive factor within the SSC ($P = 0.002$).

One-Year Follow-Up

In eight patients (50%), FLIO measurement was repeated after a time interval of 12 months. After this time, BCVA did not show significant deterioration compared with the baseline measurement ($P = 0.86$), although six of eight patients reported mild decline of their vision. Color fundus images and FAF images revealed different degrees of increase of hyperfluorescent flecks and the area of atrophic lesions. Individual flecks with short fluorescence lifetimes (red) were observed to transform to long lifetimes (blue) (Fig. 4, red arrow). During the study period, additional flecks with long lifetime values appeared. Although mean fluorescence lifetime values of the analyzed ETDRS areas featured slightly longer lifetimes, the difference within 1 year was not statistically significant (SSC: $P = 0.07$; LSC: $P = 0.21$).

Correlation of Fluorescence Lifetimes and Visual Acuity

Assessed mean fluorescence lifetime values from the central area of the ETDRS grid were correlated with BCVA (Fig. 3B).

Short fluorescence lifetimes were associated with a higher ETDRS letter score than long fluorescence lifetimes in both channels. Significant correlation was found between BCVA (ETDRS letters) and fluorescence decay times in both spectral channels (SSC: $r^2 = 0.34$, $P = 0.0005$; LSC: $r^2 = 0.29$, $P = 0.0014$).

Analysis of Individual Fluorescence Lifetime Components

The individual lifetimes $T1$ and $T2$ (short and long decay components), which were used for calculation of the mean fluorescence lifetime value Tm in the SSC and LSC (see Equation 1), were further analyzed. Therefore, distribution histograms $T1$ against $T2$ were depicted for each channel (Fig. 5).

In the healthy fundus, four lifetime clouds were clearly identifiable (Fig. 5A): the principle lifetime cloud was built by the neurosensory retina, whereas the central macula featured shorter lifetime parameters, especially of $T1$ and the retinal vessels, and the optic nerve head showed longer lifetime components $T2$.

Hyperfluorescent flecks with long fluorescence lifetimes in Stargardt patients were well discernible from other retinal structures and featured longer lifetime components $T1$,

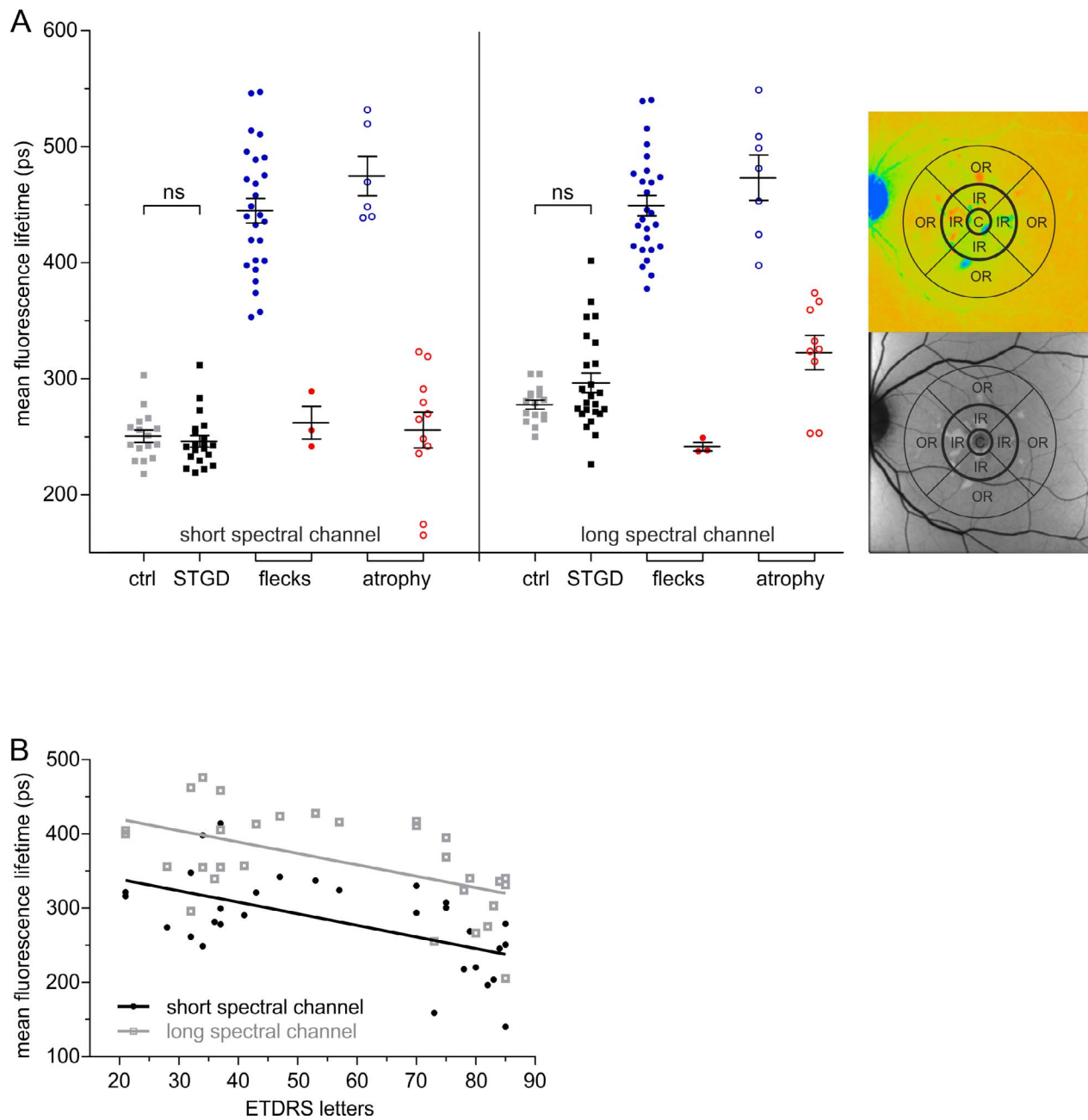


FIGURE 3. (A) Quantitative analysis of retinal autofluorescence lifetimes in patients with STGD. Mean fluorescence lifetime values were evaluated within the ETDRS grid shown (diameter central area $c = 1$ mm, inner ring IR = 3 mm, outer ring OR = 6 mm). The following areas within the inner ETDRS ring were analyzed: hyperfluorescent spots (●) and atrophic areas (○) with short or long fluorescence lifetimes and surrounding retinal tissue (▲). Mean values from the short and the long spectral channel were compared with the healthy retina within the inner ETDRS ring in healthy control eyes (■) ($n = 32$ in the affected eyes and $n = 15$ in the control eyes; short spectral channel = 498–560 nm, long spectral channel = 560–720 nm; ns, not significant). (B) Correlation of mean fluorescence lifetime with BCVA (ETDRS letters) for the short spectral channel (black circle, 498–560 nm; $r^2 = 0.34$, $P = 0.0005$) and the long spectral channel (gray square, 560–720 nm; $r^2 = 0.29$, $P = 0.0014$).

whereas T_2 remained largely unchanged (Fig. 5B). Patients with additional short lifetime flecks (Fig. 5C) featured a corresponding lifetime cloud that was characterized by shorter T_1 than the surrounding retina. Atrophic areas were characterized by a shift of the parameter T_2 to longer values (Fig. 5D).

FLIO Measurements In Vitro

atRAL and A2E, as a component of lipofuscin, exhibited strong autofluorescence, especially in the LSC (560–720 nm). Mean

fluorescence lifetimes of A2E were between 350 and 450 ps in the SSC and between 220 and 250 ps in the LSC. Fluorescence decay time measurement of atRAL revealed extremely short lifetimes T_m , T_1 , and T_2 (LSC: $T_m = 38$ ps). Fluorescence lifetimes and distribution did not change by modifying the concentration of the solution. Retinal, as a strong fluorophore, dominated lifetime and distribution histograms in mixed solutions, leading to a shift toward short lifetimes (Supplementary Fig. S1).

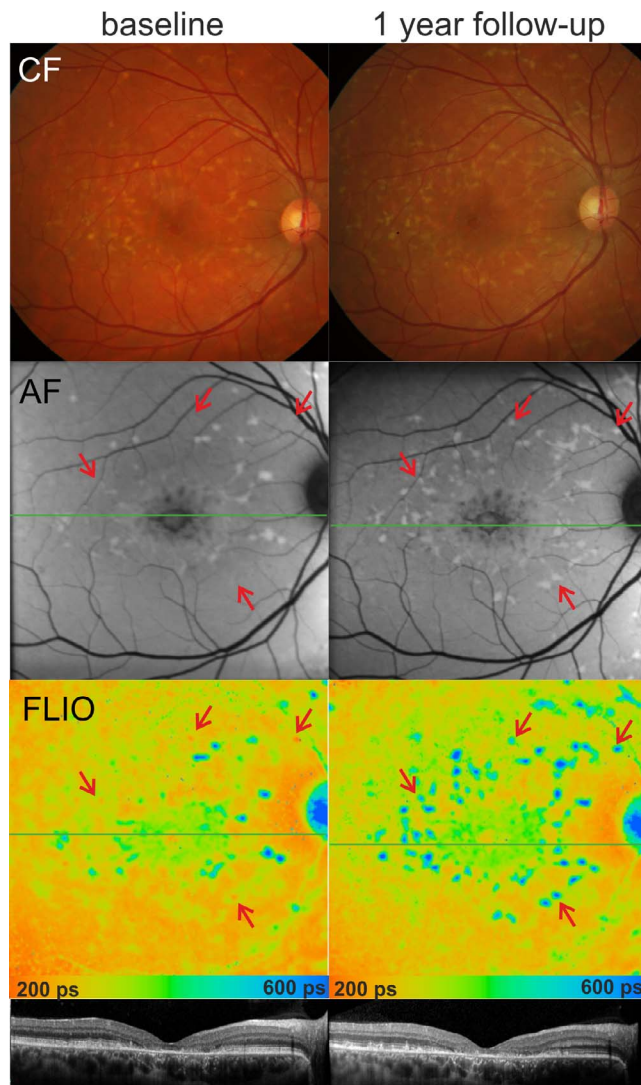


FIGURE 4. Disease progression within 1 year (patient 2). Color fundus (CF), fundus AF, and FLIO (long spectral channel) with indicated lines of the optical coherence tomography scan (OCT) (baseline, *left*). A 1-year follow-up examination (*right*) shows clear disease progression with accumulation of hyperfluorescent flecks. The *red arrows* mark areas with short fluorescence lifetimes that converted to long lifetimes within 1 year.

DISCUSSION

In the current study, we used a fluorescence lifetime imaging ophthalmoscope for investigation of lifetime characteristics of endogenous retinal fluorophores in patients with STGD. Whereas areas without flecks and atrophy secondary to STGD featured lifetime values comparable to age-matched healthy controls, both hyperfluorescent flecks and hypofluorescent atrophic lesions showed either shorter or longer lifetime values.

There are various bis-retinoid pigments that can be identified by mass spectroscopy and chromatography. All of these components derive from aRAL that is released from opsin after photoisomerization of ground state 11-*cis*-retinal following capture of a photon of light (for a review see Ref. 31). It has been shown that aRAL accumulates in photoreceptor outer segments in patients with STGD.³² STGD is caused by dysfunction of ABCR, which transports aRAL from the inside to the outside of disc membranes. This leads to an

accumulation of aRAL condensation products and subsequently to degeneration of RPE and photoreceptors. Using picosecond fluorometry, the lifetime (T_l) of aRAL was shown to be 31 ps.³² Our own measurements of pure retinal, using an excitation wavelength of 473 nm, revealed mean fluorescence decay times T_m of 38 ps in the emission channel between 560 and 720 nm. However, retinal is only an intermediate product and is rapidly reduced to aRAL by the retinol dehydrogenase and further transformed to secondary products such as A2E.³³

In FLIO measurements of patients with STGD, we found a vast range of fluorescence lifetimes within STGD lesions. Most hyperfluorescent flecks, suggested to contain lipofuscin as a major component, displayed longer lifetimes than the surrounding retina. The long fluorescence may also indicate a major dysfunction of the underlying RPE due to accumulation of lipofuscin and insufficient degradation. However, unexpectedly, we found STGD lesions with the same appearance in the autofluorescence intensity profile, displaying shorter lifetimes than the surrounding retina. Our follow-up fluorescence lifetime measurements suggest that the short lifetime lesions may turn into lesions displaying the characteristic long lifetimes. It can only be speculated at this point whether fluorophores from the retinoid cycle within the early flecks cause these short lifetimes. Further studies *ex vivo* and in suitable animal models, such as the *Abca4*^{-/-} mouse, are needed to dissect the contributors of retinal lifetimes and to evaluate whether the appearance of short lifetime lesions serves as a marker for disease progression and may be used to monitor therapeutic approaches. Another powerful tool to study disease progression is the two-dimensional (2D) plotting of the short and long lifetime components (Fig. 5). Here, we show that specific retinal areas like the macular center, the neuronal retina, the retinal vessels, and the optic nerve head were clearly discernible within the 2D plot in the healthy retina. This indicates that different fluorophores with distinct decay characteristics, represented by the short and the long decay components T_1 and T_2 , contribute to the mean fluorescence lifetime T_m . In STGD, additional areas were identifiable, corresponding to hyperfluorescent areas with short or long fluorescence lifetimes and to areas with geographic atrophy. FLIO potentially provides additional information about the content and conformation of endogenous fluorophores that could be used for monitoring of retinal metabolic changes over the course of disease. By analyzing lifetime data of *in vitro* measurements of aRAL and A2E and comparing with *in vivo* FLIO data, one hypothesis could be that retinal contributes to short fluorescence lifetimes within hyperfluorescent lesions. Another possibility is that A2E, which is a byproduct of the visual cycle and has short lifetimes of approximately 250 ps, contributes to short lifetimes seen in early flecks. On the other hand, high concentrations of other lipofuscin components potentially originating from cell detritus and stacked cells might lead to prolonged fluorescence decay time in longer standing flecks. However, caution is needed when extrapolating observations from *ex vivo* measurements into *in vivo* conditions in the retina, as the fluorescence lifetime signal *in vivo* derives from various endogenous fluorophores. A recent study on near-infrared AF and short-wavelength (SW) AF suggests that the RPE cell layer might already be altered or lost in early stages of fleck formation. Thereby, the increased SW AF signal within flecks might originate from augmented lipofuscin formation within degenerating photoreceptor outer and inner segments secondary to RPE atrophy.³⁴

Interestingly, we did not find any differences in mean retinal fluorescence lifetime values in areas of the fundus without flecks of patients with STGD compared with age-matched healthy controls, even though generally higher AF intensities are expected in STGD.¹¹ This supports the hypothesis that the

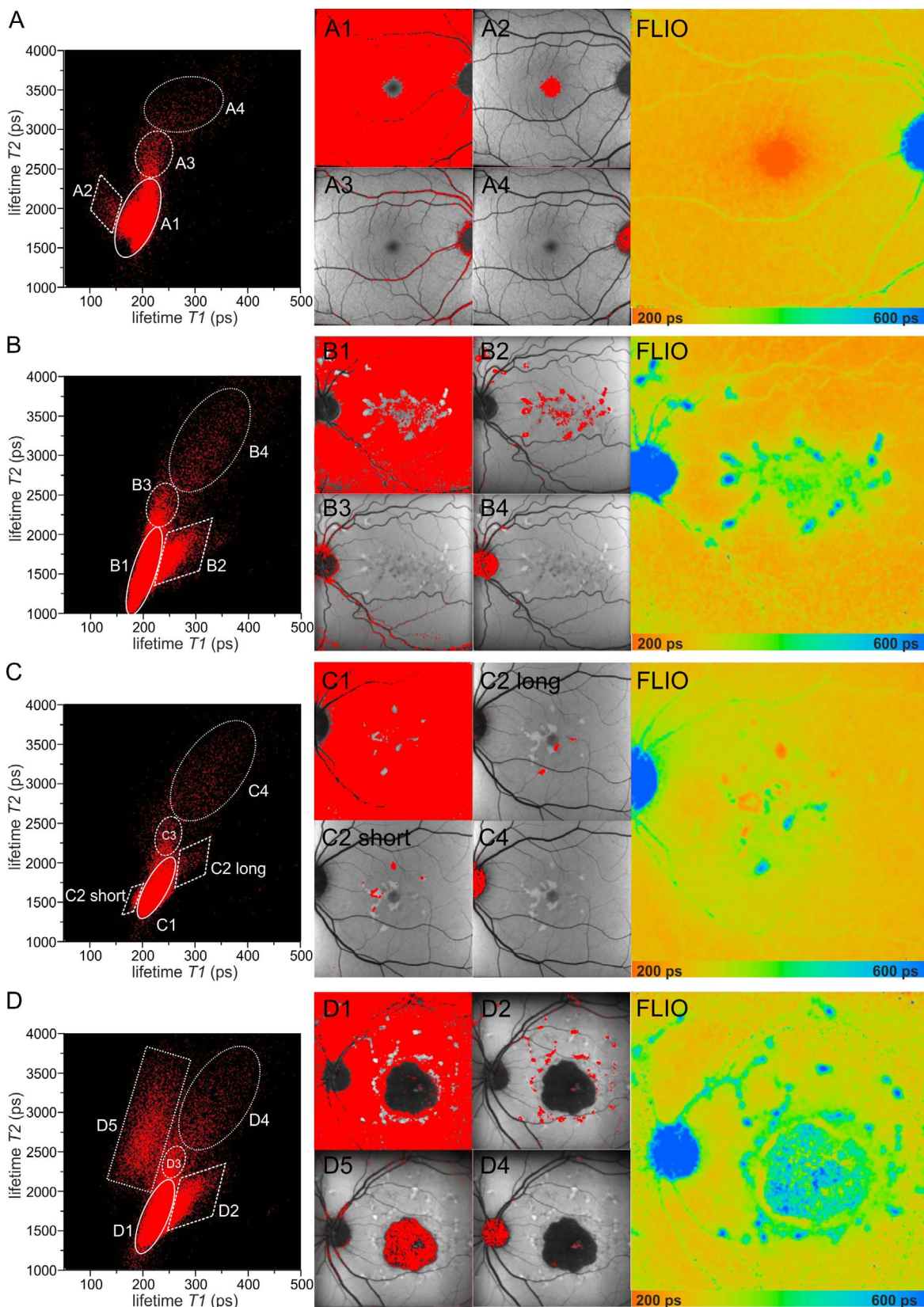


FIGURE 5. Distribution of the short versus long fluorescence lifetime components $T1$ and $T2$. Distribution histograms with corresponding FLIO (long spectral channel) are shown for a healthy 36-year-old subject (A), a Stargardt patient with long lifetime flecks (patient 3) (B), a Stargardt patient with short and long lifetime flecks (patient 11) (C), and a Stargardt patient with central geographic atrophy (patient 10) (D). Specific areas are highlighted according to the lifetime distribution clouds: normal retina (A1, B1, C1, D1), macular center (A2), retinal vessels (A3, B3, C3, D3), optic nerve head (A4, B4, C4, D4), hyperfluorescent flecks (B2, C2, D2), and atrophic retinal area (D5).

main fluorescence of the retina originates from components of the visual cycle, mainly lipofuscin, within the RPE.^{10,14,20} As fluorescence lifetimes are not dependent on the fluorophore concentration, we did not expect any changes in fluorescence lifetimes in cases with increased fluorescence intensity as seen in STGD.^{25,35} Probably, retinal fluorescence indicates an equilibrium of short and long decay components that is not changed by equal increase of the components. On the other hand, in areas with strongly increased autofluorescence intensity, lifetimes can be shifted toward shorter or longer lifetimes depending on the predominant fluorophore of the lesions. This differentiation is an important finding, as it might be used to assess disease activity and serve as control for future therapies in the field of gene therapy and stem cell approaches. Functionality of RPE cells might be quantified, and early imbalance and dysfunction might be detected. However, there is some controversy on lipofuscin toxicity. In particular, it is unclear whether RPE degeneration is caused by excessive lipofuscin accumulation or whether excessive lipofuscin accumulation is caused by impaired autophagy and recycling of retinoids by compromised RPE function.¹⁸

Atrophic lesions in STGD typically showed strongly decreased autofluorescence intensity but were characterized by both short and long fluorescence decay times. As the intact retinal structure with preserved RPE contributes to short decay times, the long lifetimes could be explained by the loss of the retinal architecture and increased influence of underlying structures such as the choroid. On the other hand, the short lifetimes within atrophic areas were predominantly seen in the central macular area, and given recent observations linking macular pigment to short lifetimes, they are likely to originate from macular pigment.³⁶ However, the distribution of this pigment seems to be strongly altered due to the underlying disease and the destruction of the retinal layer architecture, and therefore, this may be another marker for disease progression.

This study has some limitations, which include the number of patients measured and the naturally occurring heterogeneity of the phenotypic appearance. Furthermore, a longer follow-up time is necessary to confirm and refine FLIO markers for disease progression of STGD. The diagnosis of STGD for this study relies on the clinical assessment.

CONCLUSIONS

Analysis of retinal fluorescence lifetimes can be used to characterize and differentiate hyperfluorescent lesions and hypofluorescent atrophic areas in STGD. The change of lifetimes over time may provide a useful tool to predict disease progression and may be used to assess therapeutic effects in upcoming clinical trials for STGD.

Acknowledgments

The authors thank Janet R. Sparrow, PhD (Department of Ophthalmology, Columbia University, New York, NY, USA), for providing the A2E stock solution. The authors thank Jörg Fischer, PhD, Yoshihiko Katayama, PhD, and Kester Nahen, PhD, from Heidelberg Engineering GmbH, Heidelberg, Germany, for providing technical assistance for the FLIO device.

Supported by Swiss National Science Foundation Grant 320030_156019. The sponsor or funding organization had no role in the design or conduct of this research.

Disclosure: **C. Dysli**, Heidelberg Engineering (F); **S. Wolf**, Heidelberg Engineering (F); **K. Hatz**, None; **M.S. Zinkernagel**, Heidelberg Engineering (F)

References

1. Rotenstreich Y, Fishman GA, Anderson RJ. Visual acuity loss and clinical observations in a large series of patients with Stargardt disease. *Ophthalmology*. 2003;110:1151-1158.
2. Armstrong JD, Meyer D, Xu S, Elfervig, JL. Long-term follow-up of Stargardt's disease and fundus flavimaculatus. *Ophthalmology*. 1998;105:448-457. discussion 457-458.
3. Fishman GA, Farber M, Patel BS, Derlacki DJ. Visual acuity loss in patients with Stargardt's macular dystrophy. *Ophthalmology*. 1987;94:809-814.
4. Kim LS, Fishman GA. Comparison of visual acuity loss in patients with different stages of Stargardt's disease. *Ophthalmology*. 2006;113:1748-1751.
5. Allikmets R, Singh N, Sun H, et al. A photoreceptor cell-specific ATP-binding transporter gene (ABCR) is mutated in recessive Stargardt macular dystrophy. *Nat Genet*. 1997;15:236-246.
6. Molday LL, Rabin AR, Molday RS. ABCR expression in foveal cone photoreceptors and its role in Stargardt macular dystrophy. *Nat Genet*. 2000;25:257-258.
7. Schmidt S, Postel EA, Agarwal A, et al. Detailed analysis of allelic variation in the ABCA4 gene in age-related maculopathy. *Invest Ophthalmol Vis Sci*. 2003;44:2868-2875.
8. Webster AR, Héon E, Lotery AJ, et al. An analysis of allelic variation in the ABCA4 gene. *Invest Ophthalmol Vis Sci*. 2001;42:1179-1189.
9. Lewis RA, Shroyer NF, Singh N, et al. Genotype/phenotype analysis of a photoreceptor-specific ATP-binding cassette transporter gene, ABCR, in Stargardt disease. *Am J Hum Genet*. 1999;64:422-434.
10. Delori FC, Staurengi G, Arend O, Dorey CK, Goger DG, Weiter JJ. In vivo measurement of lipofuscin in Stargardt's disease: *Fundus flavimaculatus*. *Invest Ophthalmol Vis Sci*. 1995;36:2327-2331.
11. Burke TR, Duncker T, Woods RL, et al. Quantitative fundus autofluorescence in recessive Stargardt disease. *Invest Ophthalmol Vis Sci*. 2014;55:2841-2852.
12. Glazer LC, Dryja TP. Understanding the etiology of Stargardt's disease. *Ophthalmol Clin North Am*. 2002;15:93-100.
13. Delori FC, Goger DG, Dorey CK. Age-related accumulation and spatial distribution of lipofuscin in RPE of normal subjects. *Invest Ophthalmol Vis Sci*. 2001;42:1855-1866.
14. Delori FC, Dorey CK, Staurengi G, Arend O, Goger DG, Weiter JJ. In vivo fluorescence of the ocular fundus exhibits retinal pigment epithelium lipofuscin characteristics. *Invest Ophthalmol Vis Sci*. 1995;36:718-729.
15. Duncker T, Greenberg JP, Ramachandran R, et al. Quantitative fundus autofluorescence and optical coherence tomography in best vitelliform macular dystrophy. *Invest Ophthalmol Vis Sci*. 2014;55:1471-1482.
16. Duncker T, Lee W, Tsang SH, et al. Distinct characteristics of inferonasal fundus autofluorescence patterns in Stargardt disease and retinitis pigmentosa. *Invest Ophthalmol Vis Sci*. 2013;54:6820-6826.
17. Ablonczy Z, Higbee D, Anderson DM, et al. Lack of correlation between the spatial distribution of A2E and lipofuscin fluorescence in the human retinal pigment epithelium. *Invest Ophthalmol Vis Sci*. 2013;54:5535-5542.
18. Ach T, Huisingh C, McGwin G Jr, et al. Quantitative autofluorescence and cell density maps of the human retinal pigment epithelium. *Invest Ophthalmol Vis Sci*. 2014;55:4832-4841.
19. Rudolf M, Vogt SD, Curcio CA, et al. Histologic basis of variations in retinal pigment epithelium autofluorescence in eyes with geographic atrophy. *Ophthalmology*. 2013;120:821-828.

20. Lois N, Halfyard AS, Bird AC, Holder GE, Fitzke FW. Fundus autofluorescence in Stargardt macular dystrophy: *Fundus flavimaculatus*. *Am J Ophthalmol*. 2004;138:55–63.
21. Gomes NL, Greenstein VC, Carlson JN, et al. A comparison of fundus autofluorescence and retinal structure in patients with Stargardt disease. *Invest Ophthalmol Vis Sci*. 2009;50:3953–3959.
22. Sunness JS, Steiner JN. Retinal function and loss of autofluorescence in Stargardt disease. *Retina*. 2008;28:794–800.
23. McBain VA, Townend J, Lois N. Progression of retinal pigment epithelial atrophy in Stargardt disease. *Am J Ophthalmol*. 2012;154:146–154.
24. Duncker T, Marsiglia M, Lee W, et al. Correlations among near-infrared and short-wavelength autofluorescence and spectral-domain optical coherence tomography in recessive Stargardt disease. *Invest Ophthalmol Vis Sci*. 2014;55:8134–8143.
25. Becker W. Fluorescence lifetime imaging—techniques and applications. *J Microsc*. 2012;247:119–136.
26. Dysli C, Queller G, Abegg M, et al. Quantitative analysis of fluorescence lifetime measurements of the macula using the fluorescence lifetime imaging ophthalmoscope in healthy subjects. *Invest Ophthalmol Vis Sci*. 2014;55:2106–2113.
27. Dysli C, Wolf S, Zinkernagel MS. Fluorescence lifetime imaging in retinal artery occlusion. *Invest Ophthalmol Vis Sci*. 2015;56:3329–3336.
28. Fishman GA, Stone EM, Grover S, Derlacki DJ, Haines HL, Hockey RR. Variation of clinical expression in patients with Stargardt dystrophy and sequence variations in the ABCR gene. *Arch Ophthalmol*. 1999;117:504–510.
29. International Electrotechnical Commission (IEC). International Standard 60825-1:2007 (Edition 2, ISBN 2-8318-9085-3)/60825-1:2014 (Edition 3, ISBN 978-2-8322-1499-2). *International Electrotechnical Commission*, TC 76, ICS 13.110, ICS 31.260.
30. Laser Institute of America. *ANSI Z136.1—2007 American National Standard for Safe Use of Lasers*. Orlando, FL: Laser Institute of America; 2007.
31. Sparrow JR, Gregory-Roberts E, Yamamoto K, et al. The bisretinoids of retinal pigment epithelium. *Prog Retin Eye Res*. 2012;31:121–135.
32. Loguinova MY, Zagidullin VE, Feldman TB, et al. Spectral characteristics of fluorophores formed via interaction between all-trans-retinal with rhodopsin and lipids in photoreceptor membrane of retina rod outer segments. *Biochemistry (Moscow) Suppl Ser A: Membrane Cell Biol*. 2009;3:134–143.
33. Masutomi K, Chen C, Nakatani K, Koutalos Y. All-trans retinal mediates light-induced oxidation in single living rod photoreceptors. *Photochem Photobiol*. 2012;88:1356–1361.
34. Sparrow JR, Marsiglia M, Allikmets R, et al. Flecks in recessive Stargardt disease: short-wavelength autofluorescence, near-infrared autofluorescence, and optical coherence tomography. *Invest Ophthalmol Vis Sci*. 2015;56:5029–5039.
35. Bastiaens PI, Squire A. Fluorescence lifetime imaging microscopy: spatial resolution of biochemical processes in the cell. *Trends Cell Biol*. 1999;9:48–52.
36. Sauer L, Schweitzer D, Ramm L, Augsten R, Hammer M, Peters S. Impact of macular pigment on fundus autofluorescence lifetimes. *Invest Ophthalmol Vis Sci*. 2015;56:4668–4679.